New Phosphacyclic Diphosphines for Rhodium-Catalyzed Hydroformylation

Lars A. van der Veen, Paul C. J. Kamer, and Piet W. N. M. van Leeuwen*

Institute of Molecular Chemistry, University of Amsterdam, Nieuwe Achtergracht 166, 1018 WV Amsterdam, The Netherlands

Received July 7, 1999

The use of phosphacyclic diphosphines based on the xanthene backbone as ligands in rhodium-catalyzed hydroformylation was studied. New phosphacyclic xantphos ligands with wide natural bite angles were synthesized, and a short, efficient route toward the synthesis of 10-chlorophenoxaphosphine and 10-chlorophenothiaphosphine was developed. The effect of the phosphacyclic moieties on the coordination chemistry in the (diphosphine)$Rh(CO)_2H$ complexes was investigated using NMR and IR spectroscopy. Both NMR and IR spectroscopy showed that the phosphacyclic xantphos ligands exhibit an enhanced preference for diequatorial (ee) chelation compared to the diphenylphosphino-substituted parent compound. In the hydroformylation of 1-octene the introduction of the phosphacyclic moieties leads to higher reaction rates. More importantly, the dibenzophospholyl- and phenoxaphosphino-substituted xantphos ligands exhibit an unprecedented high activity and selectivity in the hydroformylation of trans 2- and 4-octene to *linear* nonanal. The high activities of the phosphacyclic xantphos ligands are explained by the lower phosphine basicity and the wider natural bite angles of the phosphacyclic ligands. The extraordinary high activity of the phenoxaphosphino-substituted xantphos ligand can be attributed to the 4- to 6-fold higher rate of CO dissociation compared to the other xantphos ligands. CO dissociation rates from the (diphosphine)$Rh(CO)_2H$ complexes were determined using ^{13}CO labeling in rapid-scan IR experiments.

Introduction

Rhodium-catalyzed hydroformylation is one of the world's largest homogeneously catalyzed processes in industry.[1−3] The key issue in this process, where linear aldehydes are the most desired products, is the control of regioselectivity. Since the stereoelectronic properties of ligands have a pronounced influence on the catalytic performance, a wide variety of ligands have been synthesized and tested in the hydroformylation reaction. Among the different classes of compounds, phosphines are the most widely used ligands.

The generally accepted, dissociative mechanism for rhodium triphenylphosphine-catalyzed hydroformylation as proposed by Wilkinson is shown in Scheme 1.[4] The active catalyst is a trigonal bipyramidal hydridorhodium complex, which usually contains two phosphorus donor ligands. Under moderate reaction conditions, the rate-limiting step in the catalytic cycle is often the displacement of a carbonyl ligand by the incoming alkene. The regiochemistry of the reaction is determined by the mode of alkene insertion in the hydridorhodium complex. The linear $L_2Rh(CO)(alkyl)$ species will result in formation of the linear aldehyde, while the branched $L_2Rh(CO)(alkyl)$ species can either give the branched aldehyde or, via β-hydride elimination, give rise to alkene isomerization.

The trigonal bipyramidal rhodium complexes containing two coordinated triphenylphosphine ligands can exist in two isomeric forms, in which the phosphine ligands coordinate in a diequatorial (ee) or a equatorial−apical (ea) fashion.[5] At room temperature these isomers are in rapid equilibrium with an ee:ea ratio of 85:15. Diphosphine ligands can in principle stabilize either one of the two isomers, depending on the bridge between the two phosphine moieties. This so-called ligand backbone restricts the P−M−P bite angle, and therefore the conformation of the rhodium−diphosphine complexes, to specific geometries.

Structures ee and ea

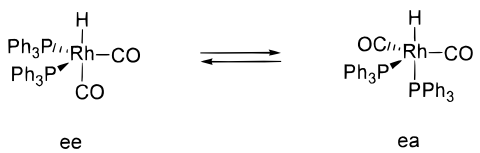

ee ea

Casey and Whiteker have developed the concept of the natural bite angle to calculate the preferred chelation angle of diphosphine ligands using molecular

(1) Parshall, G. W. *Homogeneous Catalysis: The Applications and Chemistry of Catalysis by Soluble Transition Metal Complexes*; Wiley: New York, 1980.

(2) Beller, M.; Cornils, B.; Frohning, C. D.; Kohlpaintner, C. W. *J. Mol. Catal. A: Chem.* **1995**, *104*, 17−85.

(3) Frohning, C. D.; Kohlpaintner, C. W. In *Applied Homogeneous Catalysis with Organometallic Compounds: A Comprehensive Handbook in Two Volumes*; Cornils, B., Herrmann, W. A., Eds.; VCH: Weinheim, 1996; Vol. 1, Chapter 2, pp 27−104.

(4) Evans, D.; Osborn, J. A.; Wilkinson, G. *J. Chem. Soc. A* **1968**, 3133−3142.

(5) Brown, J. M.; Kent, A. G. *J. Chem. Soc., Perkin Trans. 2* **1987**, 1597−1607.

10.1021/om990523j CCC: $18.00
Publication on Web 10/13/1999

Scheme 1

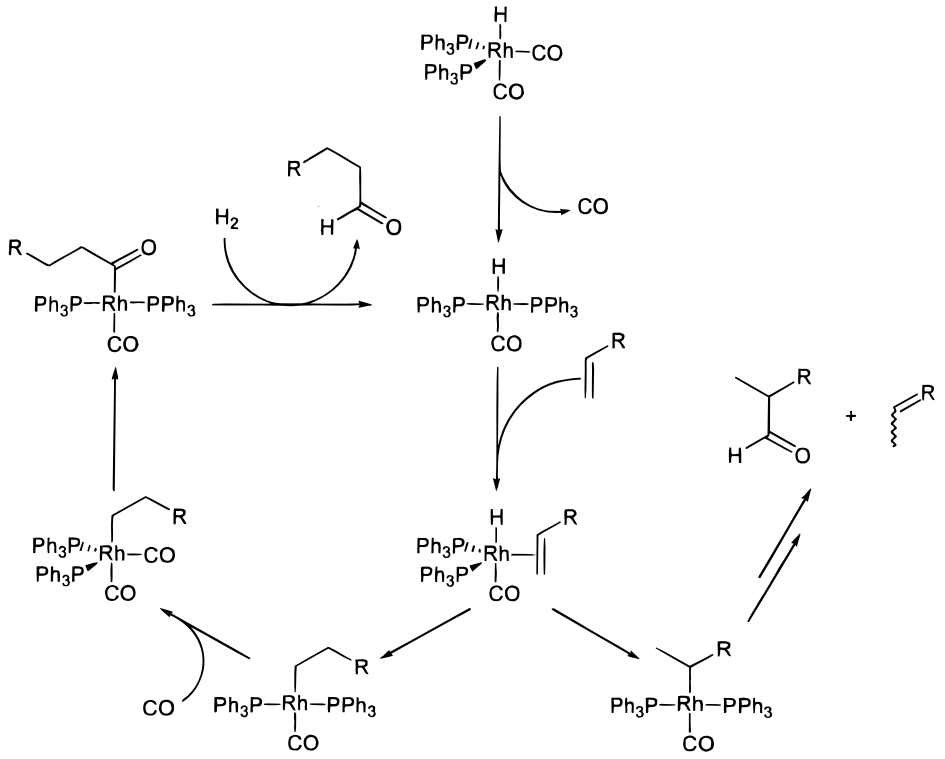

mechanics.[6] They were the first to show that the bite angle has a great influence on the regioselectivity in the rhodium-catalyzed hydroformylation.[7] Using BISBI, an ee coordinating diphosphine with a wide natural bite angle of approximately 113°, a linear-to-branched (l:b) aldehyde ratio of 66:1 was obtained, while the ea coordinating diphosphine dppe with a narrow natural bite angle of 85° gave a l:b ratio of only 2:1. To investigate the exact nature of the bite angle effect, we have developed a series of diphosphine ligands based on the xanthene-type backbones (Figure 1).[8,9] In this series of ligands, a clear trend of increasing selectivity for linear aldehyde formation with increasing natural bite angle was observed.

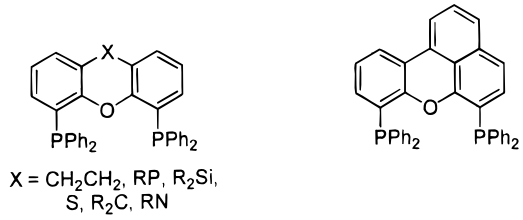

Figure 1. Xantphos family.

On the basis of these results it was concluded that for inducing high regioselectivity in the rhodium-catalyzed hydroformylation diphosphine ligands with wide natural bite angles are required. In our effort to develop new ligands with wide natural bite angles, we discovered that not only the variation of the ligand backbone but also substitution of the standard diphenylphosphine moieties have a direct influence on the ligand bite angle. Molecular mechanics calculations revealed that the introduction of phosphacyclic moieties on the xanthene backbone yields diphosphine ligands with bite angles of 120−126° (Figure 2, Table 1). Herein we describe the synthesis of new phosphacyclic ligands, their coordination chemistry in the (diphosphine)Rh-$(CO)_2H$ complexes, and their catalytic performance in the hydroformylation of 1-octene. The phosphacyclic xantphos derivatives show an increased preference for ee coordination and display a higher activity in the hydroformylation of 1-octene than the noncyclic parent ligand. Moreover, DBP−xantphos (**2**) and POP−xantphos (**5**) give very active and selective catalysts for the hydroformylation of internal octenes to linear nonal.[10] The very high hydroformylation and isomerization activity of ligand **5** is the direct result of an enhanced rate of CO dissociation from the (diphosphine)$Rh(CO)_2H$ complex, which was measured using ^{13}CO labeling in rapid-scan IR experiments.

Results

Synthesis. The ligands **1**−**3**, **5**, and **6** were prepared by dilithiation of 4,5-dibromo-2,7-di-*tert*-butyl-9,9-dimethylxanthene (**8**) with *n*-butyllithium at −60 °C, followed by reaction with the corresponding chlorophosphines (Scheme 2). Ligand **4** was prepared by a slightly modified procedure, in which the intermediate dilithio species was converted into the dizinc compound before it was made to react with 10-chlorophosphorine. This way the occurrence of deprotonation of the methylene group at the 9-position of the phosphorine ring is

(6) Casey, C. P.; Whiteker, G. T. *Isr. J. Chem.* **1990**, *30*, 299−304.
(7) Casey, C. P.; Whiteker, G. T.; Melville, M. G.; Petrovich, L. M.; Gavney, J. A., Jr.; Powell, D. R. *J. Am. Chem. Soc.* **1992**, *114*, 5535−5543.
(8) Kranenburg, M.; van der Burgt, Y. E. M.; Kamer, P. C. J.; van Leeuwen, P. W. N. M. *Organometallics* **1995**, *14*, 3081−3089.
(9) van der Veen, L. A.; Keeven, P. H.; Schoemaker, G. C.; Reek, J. N. H.; Kamer, P. C. J.; van Leeuwen, P. W. N. M.; Lutz, M.; Spek, A. L. Submitted.
(10) van der Veen, L. A.; Kamer, P. C. J.; van Leeuwen, P. W. N. M. *Angew. Chem., Int. Ed.* **1999**, *38*, 336−338.

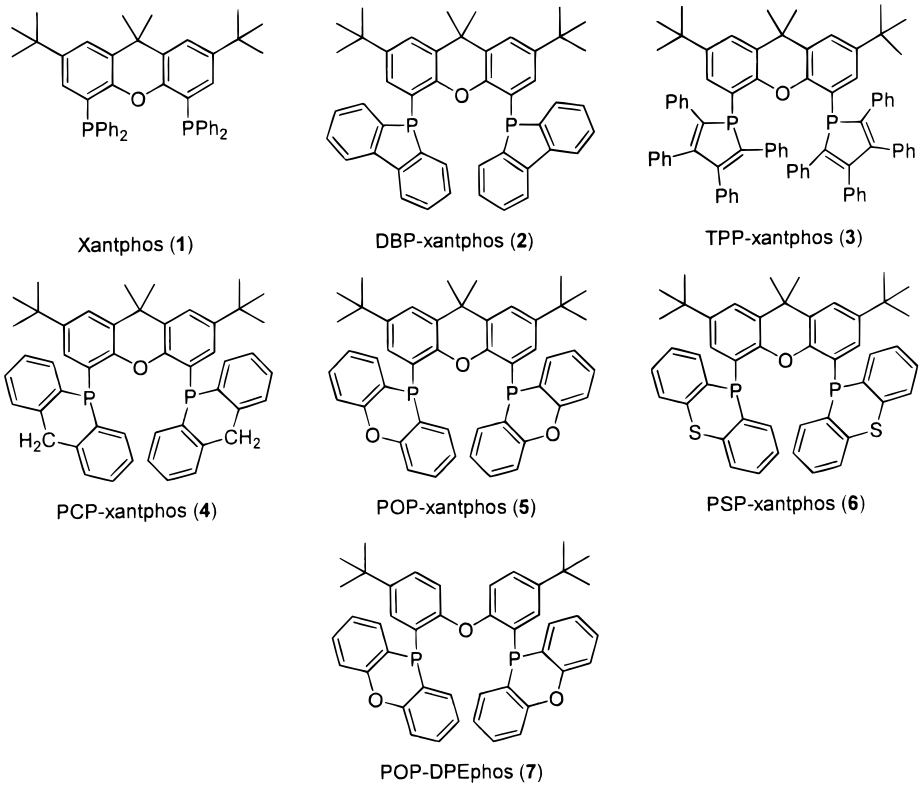

Figure 2. Phosphacyclic xantphos derivatives.

Table 1. Calculated Natural Bite Angle and Flexibility Range for the Xantphos Ligands

ligand	phosphacycle	β_n,[a] deg	flexibility range,[a] deg
di-*t*-buxantphos (**1**)		110.1	98−134
DBP−xantphos (**2**)	[*b*,*d*]dibenzophosphole	121.4	107−138
TPP−xantphos (**3**)	1,2,3,4-tetraphenyl-phosphole	124.3	111−139
PCP−xantphos (**4**)	phosphorine	123.4	108−143
POP−xantphos (**5**)	phenoxaphosphine	123.1	107−142
PSP−xantphos (**6**)	phenothiaphosphine	126.3	110−146
POP−DPEphos (**7**)	phenoxaphosphine	111.7	95−129

[a] The natural bite angle (β_n) and the flexibility range were calculated analogously to the method used by Casey and Whiteker.[6] β_n is defined as the preferred chelation angle determined only by ligand backbone constraints and not by metal valence angles. The flexibility range is defined as the accessible range of bite angles within 3 kcal mol^{-1} excess strain energy from the calculated natural bite angle.

prevented. Ligand **7** was synthesized by dilithiation of 4,4′-di-*tert*-butyldiphenyl ether (**9**) using *n*-butyllithium/TMEDA and successive reaction with 10-chlorophenoxaphosphine (**10**). 9-Chlorodibenzo[*b*,*d*]phosphole,[11] 5-chloro-1,2,3,4-tetraphenylphosphole,[11] and 10-chlorodibenzo[*b*,*e*]phosphorine[12] were prepared according to literature procedures. The synthesis of compound **10** has been reported before by Doak, Freedman, and Levy.[13] They prepared compound **10** in three steps from *o*-nitrophenyl phenyl ether by cyclodehydrohalogenation in a total yield of 17%. The low total yield of this procedure prompted us to develop a shorter and more efficient route to chlorophosphine **10**. We first prepared

Scheme 2[a]

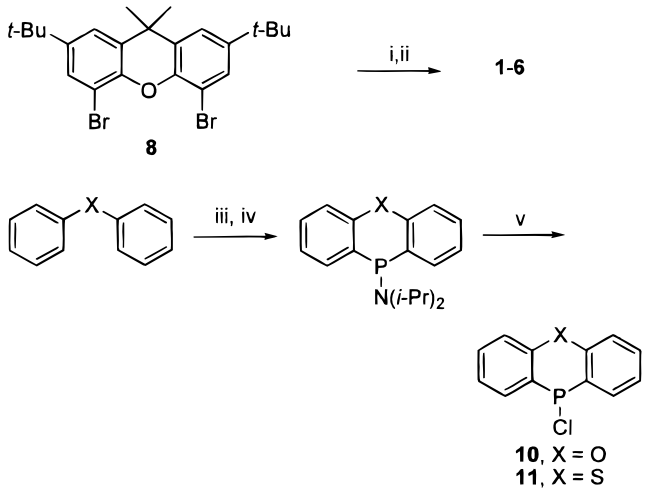

[a] (i) *n*-Buli/THF/−60 °C; (ii) ($ZnCl_2$/Et_2O/)chlorophosphine/−60 °C to rt; (iii) *n*-Buli/TMEDA/Et_2O/25 °C; (iv) (*i*-Pr)$_2$NPCl_2/hexanes/0 °C; (v) PCl_3/110 °C.

10 via a modification of the procedure developed by Teunissen and Bickelhaupt for the synthesis of 9-chlorodibenzo[*b*,*d*]phosphole.[11] This resulted in a one-step synthesis of **10** in 35% yield based on diphenyl ether. Even higher yields were obtained using a two-step procedure employing the intermediate 10-*N*,*N*-diisopropylamino-substituted phosphacycle. Both chlorophosphines **10** and **11** were synthesized by dilithiation of diphenyl ether or diphenyl sulfide using *n*-butyllithium/TMEDA, followed by reaction with *N*,*N*-diisopropylphosphoramidous dichloride, and refluxing the resulting diisopropylamine substituted phosphacycle in phosphorus trichloride. The pure products were obtained after

(11) Teunissen, H. T.; Bickelhaupt, F. *Phosphorus, Sulfur* **1996**, *118*, 309−312.
(12) de Koe, P.; Bickelhaupt, F. *Angew. Chem.* **1967**, *79*, 533−534.
(13) Doak, G. O.; Freedman, L. D.; Levy, J. B. *J. Org. Chem.* **1964**, *29*, 2382−2385.

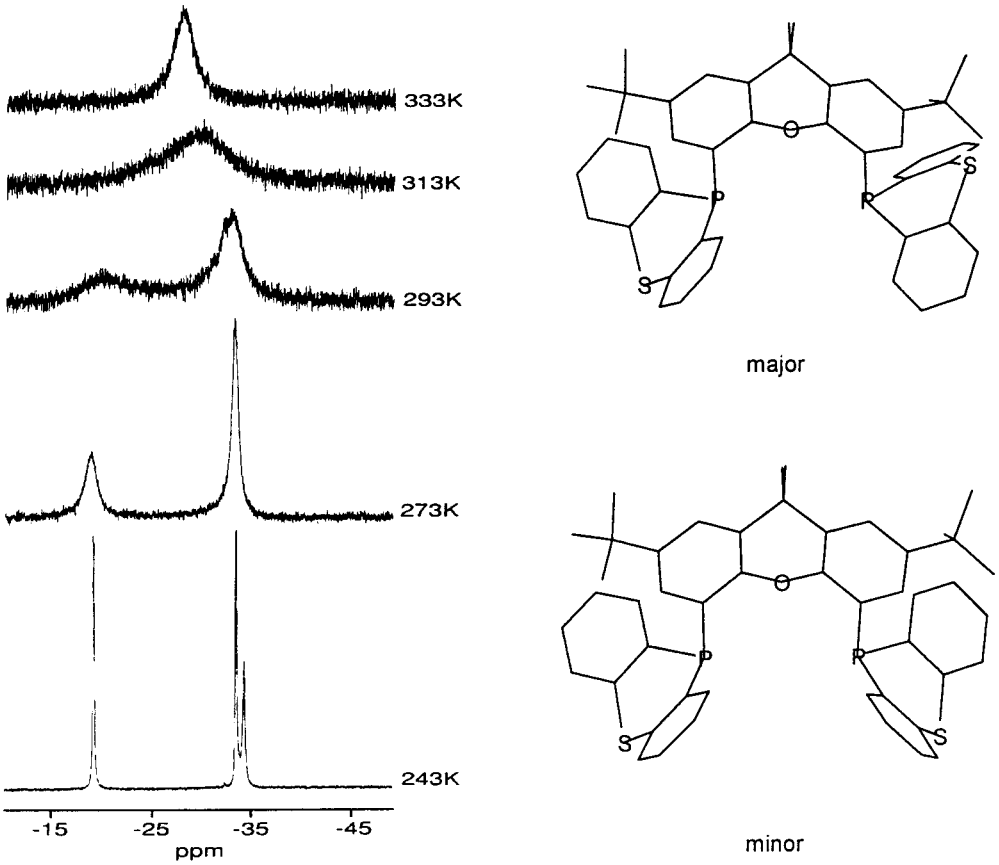

Figure 3. Variable-temperature $^{31}P\{^1H\}$ NMR spectra in $CDCl_3$ and wire models of the major and minor conformers of PSP−xantphos (**6**).

sublimation in relatively good yields of 54% and 45%, respectively.

For ligands **2**, **3**, **5**, and **7** sharp lines were observed in the NMR spectra at room temperature. Ligand **4** showed some line broadening in the ^1H and $^{31}P\{^1H\}$ NMR spectra at room temperature, probably caused by flexing of the phosphacyclic ring between two "butterfly" conformations on the NMR time scale. Due to fluxional behavior of the phenothiaphosphine moieties, only very broad signals were observed in the NMR spectra of ligand **6**. At low temperature the fluxional processes could be frozen out completely. Both in the ^1H and in the $^{31}P\{^1H\}$ NMR spectrum two different conformers of ligand **6** are observed at 223 K in a 5:2 ratio (Figure 3). The two phosphorus atoms of the major conformer are chemically different ($\Delta\delta$ = 14.3 ppm, J(P,P) = 6.7 Hz), while they are equivalent in the minor isomer. The absolute configurations of the conformers are not known, but the NMR data and molecular mechanics suggest that in the major conformer one of the phenothiaphosphine rings is pointing up, while the other ring is pointing down (Figure 3). In the minor conformer there must be a plane of symmetry, since both phosphorus atoms are identical. In this structure the butterfly conformations of the phenothiaphosphine moieties should be mirror images and both pointing down. Above 300 K the conformers rapidly interconvert on the NMR time scale by flexing one of the phenothiaphosphine rings, and only one signal is observed in the $^{31}P\{^1H\}$ NMR spectrum at −27.9 ppm.

(Diphosphine)Rh(CO)$_2$H Complexes. To determine whether the introduction of the phosphacyclic moieties on the xanthene backbone affects the chelation behavior of the xantphos ligands, we studied the solution structures of the (diphosphine)Rh(CO)$_2$H complexes, the catalyst resting state under hydroformylation conditions,[14] by NMR and IR spectroscopy. The complexes were prepared in situ from Rh(CO)$_2$(acac) and diphosphine under an atmosphere of CO/H$_2$ (1:1). The characteristic heteronuclear coupling constants for the complexes are shown in Table 2. The IR frequencies of the absorption bands of the complexes in the carbonyl region are summarized in Table 3.

Table 2. Selected NMR Data for (Diphosphine)Rh(CO)$_2$H Complexes[a]

ligand	β_n, deg	^1J(Rh,H), Hz	^1J(Rh,P), Hz	$^2J_{av}$(P,H), Hz
1	110.1	6.6	126	16.5
3	124.3	<2	138	12.2
4	123.4	3.9	135	1.8
5	123.1	2.4	151	10.4
6	126.3	3.1	140	7.7
7[b]	120.6	12.3	117	17.3/12.3

[a] In C_6D_6 at 298 K. [b] Only the ea complex isomer was observed.

For ligands **1** and **3**−**6**, the formation of the (diphosphine)Rh(CO)$_2$H complexes was evidenced by the appearance of a doublet in the $^{31}P\{^1H\}$ NMR spectra and an apparent triplet of doublets in the hydride region of the ^1H NMR spectra. For ligand **2** the (diphosphine)-Rh(CO)$_2$H complex was not formed. Instead, only the formation of the [(diphosphine)Rh(CO)$_2$]$_2$ complex was

(14) van der Veen, L. A.; Boele, M. D. K.; Bregman, F. R.; Kamer, P. C. J.; van Leeuwen, P. W. N. M.; Goubitz, K.; Fraanje, J.; Schenk, H.; Bo, C. *J. Am. Chem. Soc.* **1998**, *120*, 11616−11626.

Table 3. Selected HP−IR Data for (Diphosphine)Rh(CO)$_2$H Complexes[a]

ligand	ν_1, cm^{-1}	ν_2, cm^{-1}	ν_3, cm^{-1}	ν_4, cm^{-1}
1	2039 (m)	1996 (w)	1974 (m)	1949 (m)
3	2028 (m)		1980 (m)	1947 (vw)
4	2037 (s)	2004 (vw)	1981 (s)	1958 (w)
5	2048 (s)		1988 (s)	
6	2044 (s)	2010 (w)	1985 (s)	1963 (m)
7	2014 (vw)	2000 (s)	1973 (vw)	1962 (vs)

[a] In cyclohexane at 353 K and 20 bar of CO/H$_2$ (1:1) (carbonyl region).

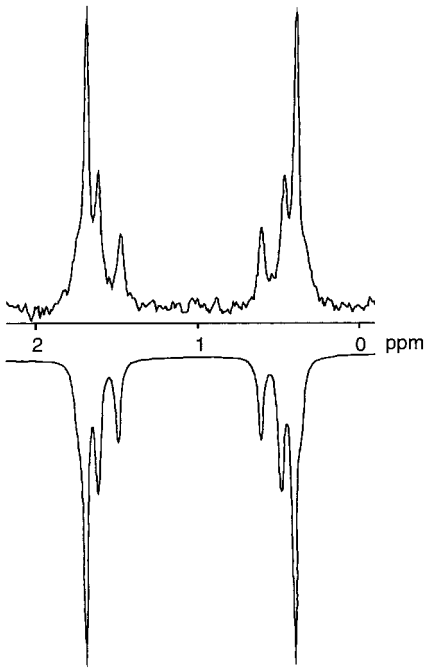

Figure 4. Observed (top) and calculated (bottom) ^{31}P{^{1}H} NMR spectrum of [(DBP−xantphos)Rh(CO)$_2$]$_2$.

observed. This dimer complex exhibits a very characteristic splitting pattern in the ^{31}P{^{1}H} NMR spectrum consistent with an AA′A″A‴XX′ spin system (^1J(Rh,P) = 149 Hz, ^2J(Rh,Rh) < 3 Hz, ^2J(Rh,P) = 10 Hz, ^3J(P,P) = −16 Hz) (Figure 4).[15,16] The IR spectrum of the complex containing ligand **2** is also typical of that of a dimer complex.[17] It exhibits two absorption bands for the terminal carbonyl ligands (2010 and 1980 cm^{-1}) and two absorption bands in the region for bridging carbonyl ligands (1797 and 1768 cm^{-1}). The dimer complex proves to be the resting state of the catalyst, since the IR spectra of the rhodium species present during a hydroformylation experiment with ligand **2** and the [(diphosphine)Rh(CO)$_2$]$_2$ complex are identical. Similar dimer complexes were also formed for ligands **5** and **7** upon long reaction times.

For ligand **7** a double doublet was observed in the ^{31}P-{^{1}H} NMR, indicating that the two phosphorus atoms in the (diphosphine)Rh(CO)$_2$H complex are not identical. The inequivalence of the phosphorus atoms indicates that only the ea isomer of the complex is formed employing this ligand. This is in good agreement with the relatively large rhodium−proton coupling constant and the relatively small rhodium−phosphorus coupling constants (vide infra). The trans phosphorus−proton coupling constant of 17.3 Hz, however, is very small for an ea complex, indicating that the complex is most likely distorted from ideal geometry. The observation of only the ea isomer in the NMR spectra of the complex with ligand **7** is confirmed by the IR spectroscopy. In the IR spectrum the intensities of the two carbonyl absorption bands of the ee complex isomer are very low compared to those of the ea isomer.[14]

The NMR data for the complexes of ligands **1** and **3**−**6** (Table 2) reveal that the introduction of the phosphacycles on the xanthene backbone leads to reduced rhodium−proton (^1J(Rh,H)) and phosphorus−proton (^2J(P,H)) coupling constants and to enhanced rhodium−phosphorus (^1J(Rh,P)) coupling constants. From previous work it is known that (diphosphine)Rh(CO)$_2$H complexes consist of mixtures of ee and ea isomers that are in dynamic equilibrium.[5,9,14] Since the fluxional behavior could not be frozen out at low temperature (163 K), estimations of the equilibrium compositions of these mixtures were obtained using the averaged phosphorus−proton coupling constants. Unfortunately, in the present series of ligands the averaged phosphorus−proton coupling constants cannot be used for quantitative estimations of the ee:ea ratios, since it is not likely that these coupling constants are exactly the same for the different phosphacycles. The rhodium−proton coupling constants in the (diphosphine)Rh(CO)$_2$H complexes, however, also prove to be indicative of the ee:ea ratio. For ea isomers of (diphosphine)Rh(CO)$_2$H complexes relatively large rhodium−proton coupling constants of 11−13 Hz are observed, while for the purely ee coordinating BISBI a coupling constant of only 2 Hz is obtained.[18] Moreover, in previous studies increasing ee:ea ratios were accompanied by decreasing rhodium−proton coupling constants.[9,14]

From the observed small rhodium−proton coupling constants for ligands **3**−**6** it can be concluded that the introduction of the phosphacycles on the xanthene backbone shifts the equilibrium composition of the (diphosphine)Rh(CO)$_2$H complexes almost completely to the ee isomer. Since the rhodium−proton coupling constant of 6.6 Hz for ligand **1** corresponds to an ee:ea isomer ratio of 7:3 (based on the phosphorus−proton coupling constant), it can be concluded that for ligands **4** and **6** the ee:ea ratio is more than 8:2. The small rhodium−proton coupling constants observed for ligands **3** and **5** indicate that these ligands coordinate almost exclusively in the ee fashion.

The effect of the phosphacycles on the ee:ea ratio is confirmed by the IR spectra of the (diphosphine)Rh-(CO)$_2$H complexes. For ligand **1** two pairs of absorption bands of comparable intensities are observed, which are assigned to the ee and the ea complex isomer.[14] In the IR spectra of the complexes of ligands **4** and **6** the intensities of the bands belonging to the ea isomer are considerably lower than those of the ee isomer. The IR spectra of the complexes of ligands **3** and **5** show only very minor contributions of the ea isomer to the complex mixture. Furthermore, Table 3 shows that on the whole

(15) James, B. R.; Mahajan, D.; Rettig, S. J.; Williams, G. M. *Organometallics* **1983**, *2*, 1452−1458.
(16) Castellanos-Páez, A.; Castillón, S.; Claver, C.; van Leeuwen, P. W. N. M.; de Lange, W. G. J. *Organometallics* **1998**, *17*, 2543−2552.
(17) Evans, D.; Yagupsky, G.; Wilkinson, G. *J. Chem. Soc. A* **1968**, 2660−2665.
(18) Boele, M. D. K.; Bregman, F. R.; Ernsting, J. M.; Muller, F.; van der Veen, L. A.; Elsevier: C. J. *J. Organomet. Chem.*, in press.

Table 4. Results of the Hydroformylation of 1-Octene at 80 °C[a]

ligand	β_n, deg	l:b ratio[b]	% linear aldehyde[b]	% isomer[b]	tof[b,c]
1	110.1	50.4 ± 1.7	94.3 ± 1.0	3.9 ± 1.0	244 ± 30
2	121.4	62.3 ± 3.4	87.8 ± 3.0	10.8 ± 3.0	453 ± 86
2[d]	121.4	47.3 ± 2.8	83.3 ± 0.1	15.0 ± 0.2	676 ± 33
3	124.3	3.7 ± 0.2	72.6 ± 1.3	7.9 ± 0.6	1332 ± 260
4	123.4	18.1 ± 0.6	90.7 ± 1.4	4.3 ± 1.3	787 ± 190
5	123.1	66.9 ± 5.4	88.7 ± 1.9	10.0 ± 1.9	1557 ± 330
6	126.3	12.8 ± 2.7	88.0 ± 2.2	4.9 ± 0.7	438 ± 72
7	111.7	2.6 ± 0.1	70.4 ± 0.9	2.3 ± 0.3	100 ± 24

[a] Conditions: $P(CO/H_2)$ (1:1) = 20 bar, ligand/Rh = 5, substrate/Rh = 637, [Rh] = 1.00 mM in toluene, number of experiments = 3. In none of the experiments was hydrogenation observed. [b]Linear over branched ratio, percent linear aldehyde, percent isomerization to 2-octene, and turnover frequency were determined at 20−30% alkene conversion. [c]Turnover frequency = (mol of aldehyde)(mol of Rh)$^{-1}$ h^{-1}. [d]$P(CO)$ = 10 bar, $P(H_2)$ = 50 bar.

the absorption bands of ligands **4**−**6** are shifted to higher wavenumbers compared to ligand **1**.

Hydroformylation of 1-Octene. The activity and selectivity of ligands **1**−**7** were tested in the hydroformylation of 1-octene. The reactions were carried out at 80 °C and 20 bar of CO/H_2 (1:1) using a 1.0 mM solution of rhodium diphosphine catalyst prepared from $Rh(CO)_2$(acac) and 5 equiv of ligand. The production of octene isomers, nonanal, and 2-methyloctanal was monitored by gas chromatography. The results of the experiments are summarized in Table 4. The averaged turnover frequencies were determined at 20−30% conversion.

The introduction of the phosphacycles on the xanthene backbone clearly results in considerably higher turnover frequencies compared to the diphenylphosphino-substituted parent ligand **1**. Especially the high activities of ligands **3** and **5** are striking. High selectivities for linear aldehyde are obtained with ligands **2** and **4**−**6**, although they are not as high as the one observed for the parent compound **1**.

Since for ligand **2** the rhodium species present under hydroformylation conditions is the [(diphosphine)Rh$(CO)_2$]$_2$ complex (vide supra), hydroformylation experiments were also performed under a 5-fold higher hydrogen pressure. Under syn gas atmosphere the catalytically inactive dimer complexes are in equilibrium with the monomeric rhodium hydride complexes.[17,19,20] Increased hydrogen pressure will shift the equilibrium in favor of the mononuclear hydridorhodium complexes, and thus this can enhance the hydroformylation rate supposing the monomer−dimer equilibrium influences the hydroformylation rate.

Monomer-dimer equilibrium

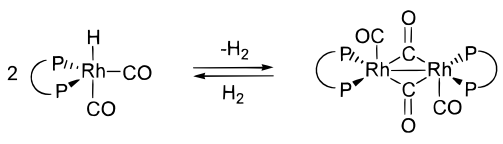

For ligand **2**, a rate enhancement of approximately 50% was observed at 50 bar of H_2. The higher hydrogen pressure also results in a slightly decreased selectivity for linear aldehyde formation.

(19) Brown, C. K.; Wilkinson, G. *J. Chem. Soc. A* **1970**, 2753−2764.
(20) Moser, W. R.; Papile, C. J.; Brannon, D. A.; Duwell, R. A.; Weininger, S. J. *J. Mol. Catal.* **1987**, *41*, 271−292.

Table 5. Results of the Hydroformylation of *trans*-2- and 4-Octene[a]

ligand	substrate	*t* (h)	% conversion[b]	l:b ratio[b]	% linear aldehyde[c]	tof[d]
(PPh_3	2-octene	1.0	8.5	0.9	46	39)
2	2-octene	1.0	10	9.5	90	65
5	2-octene	1.0	22	9.2	90	112
(PPh_3	4-octene	17	9.0	0.3	23	2.4)
2	4-octene	17	54	6.1	86	15
5	4-octene	17	67	4.4	81	20

[a] As Table 4, but at 120 °C and a constant pressure of CO/H_2 (1:1) of 2 bar and number of experiments = 2. [b]l:b ratio includes all branched aldehydes. [c]Percentage of linear aldehyde of all products other than octenes. [d]See Table 4.

Ligand **7** is not as active as the other phosphacyclic ligands. In this case substitution of the backbone with the phenoxaphosphino moieties does not lead to the large increase in activity as observed for ligand **5**. The selectivity obtained with ligand **7** is lower compared to the parent compound DPEphos and characteristic of an ea coordinating diphosphine.[7,8]

Hydroformylation of Internal Octenes. The high activities of ligands **2** and **5** in the hydroformylation of 1-octene, combined with the very high l:b ratios and the rates of isomerization to internal olefins, prompted us to test these ligands in the hydroformylation of internal octenes. The hydroformylation experiments were performed at a relatively high temperature of 120 °C and a low pressure of 2 bar CO/H_2 (1:1) to enhance the rate of isomerization and to prevent the hydroformylation of the internal alkenes. The results of the experiments are summarized in Table 5.

In the hydroformylation of trans 2-octene both ligands **2** and **5** displayed a high activity and selectivity toward the formation of the linear aldehyde. The hydroformylation of 1-octene, formed in situ by isomerization, is highly favored over the hydroformylation of the large excess of 2-octene, and no hydrogenation is observed. The high reaction temperature and the low syn gas pressure are very important for the catalytic performance of the ligands. In a preliminary experiment with ligand **5** at 100 °C and 10 bar CO/H_2 (1:1) a lower regioselectivity (l:b ratio was 6.3) and a lower activity (tof was 60) were obtained.

The high selectivity of ligands **2** and **5** is even more pronounced in the hydroformylation of trans 4-octene. Although three consecutive double-bond isomerizations have to precede hydroformylation, selectivities for linear aldehyde still exceed 80%.

Kinetics of ^{13}CO Dissociation from (Diphosphine)-Rh($^{13}CO)_2H$ Complexes. The hydroformylation results unambiguously show that the introduction of the phosphacycles on the xanthene backbone result in an increase of the hydroformylation rate. To determine in which steps in the hydroformylation cycle the introduction of the phosphacycles causes the rate enhancement, we determined the CO dissociation rates for the (diphosphine)Rh$(CO)_2H$ complexes containing ligands **4** and **5**. The CO dissociation rate constants k_1 can be obtained by exchanging ^{13}CO for ^{12}CO in the (diphosphine)Rh($^{13}CO)_2H$ complexes.[9] The CO dissociation proceeds via a dissociative mechanism and consequently obeys simple first-order kinetics. The rate constants k_1

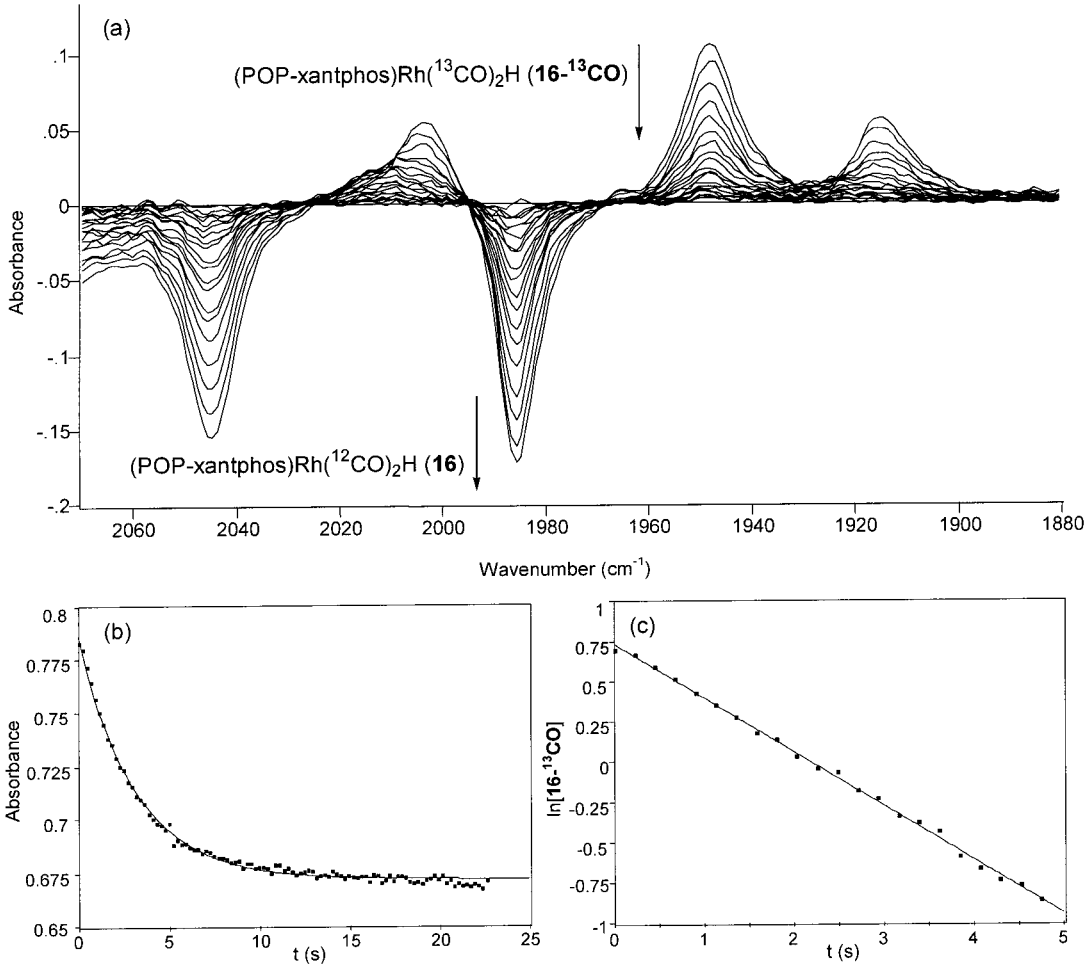

Figure 5. Representative difference IR spectrum (a) and kinetic data (b and c) for the ^{13}CO dissociation from (POP−xantphos)Rh(^{13}CO)$_2$H (**16**-^{13}CO) in the presence of unlabeled CO at 40 °C.

can, therefore, be derived from eq 1 and eq 2.

$$-\mathrm{d}[(\text{diphosphine})\mathrm{Rh}(^{13}\mathrm{CO})_2\mathrm{H})]/\mathrm{d}t = k_1[(\text{diphosphine})\mathrm{Rh}(^{13}\mathrm{CO})_2\mathrm{H})] \quad (1)$$

$$\ln[(\text{diphosphine})\mathrm{Rh}(^{13}\mathrm{CO})_2\mathrm{H})] = -k_1 t + \ln[(\text{diphosphine})\mathrm{Rh}(^{13}\mathrm{CO})_2\mathrm{H})]_0 \quad (2)$$

The (diphosphine)Rh(^{13}CO)$_2$H complexes were prepared in situ from Rh(acac)(CO)$_2$ and diphosphine under an atmosphere of ^{13}CO/H$_2$ (1:4). Complex formation was usually complete within 2 h. The exchange of ^{13}CO for ^{12}CO in the (diphosphine)Rh(^{13}CO)$_2$H complexes was monitored by rapid-scan HP IR spectroscopy at 40 °C. The ^{13}CO/^{12}CO exchange was initiated by adding a large excess of ^{12}CO (20-fold or more). The carbonyl absorptions of the complexes at approximately 1945 cm^{-1} were taken to calculate the concentrations of the complexes. These absorption bands are assigned to one of the CO vibrations of the ee isomer of the complexes. Representative kinetic data of the experiments with ligand **4** and **5** are shown in Figure 5, and the observed rate constants, k_1, are listed in Table 6.

The representative difference IR spectrum displayed in Figure 5a for one of the experiments with (POP−xantphos)Rh(^{13}CO)$_2$H (**16**-^{13}CO) clearly shows the conversion of the ^{13}CO-labeled complex in to its ^{12}CO analogue. In the IR spectrum only the ee complex isomer is visible (vide supra). The exponential decay of the intensity of the carbonyl absorption at 1948 cm^{-1} in time is displayed in Figure 5b. The solvent cyclohexane used in the experiment is responsible for the remaining background absorption of 0.67 au. The linear plot of the natural logarithm of the complex concentration (ln[Rh]) vs time (Figure 5c) is obtained by converting the background corrected absorbance in the complex concentration. The negative of the slope of this line is the first-order rate constant k_1 (eq 2).

The decay of the carbonyl resonances of the (diphosphine)Rh(^{13}CO)$_2$H complexes in time follows simple first-order kinetics in all experiments. Plots of the ln[(diphosphine)Rh(^{13}CO)$_2$H)] vs time are linear for at

Table 6. Kinetics of ^{13}CO Dissociation of (Diphosphine)Rh(^{13}CO)$_2$H Complexes[a]

ligand	phosphacycle	P(CO) (bar)	r^2	k_1 (h^{-1})
4	phosphorine	25	0.987	288 ± 8
4		25	0.987	266 ± 7
5	phenoxaphosphine	25	0.992	1188 ± 29
5		25	0.990	1171 ± 23

[a] Reaction conditions: [(diphosphine)Rh(^{13}CO)$_2$H] = 2.00 mM in cyclohexane, P(^{13}CO) = 1 bar, P(H$_2$) = 4 bar, T = 40 °C, diphosphine/Rh = 5. Values for k_1 are least-squares fit of lines from ln[Rh] vs time over the first 15 s (ligand **4**) or over the first 4 s (ligand **5**), calculated using TableCurve 2D.[38]

least 2 half-lives. Comparison of the rate constants k_1 obtained for ligands **4** and **5** with the ones obtained previously for other xantphos ligands[9] shows that the CO dissociation rate for ligand **4** is in the same range as other ligands. The CO dissociation rate for ligand **5**, however, proves to be 4−6 times as high.

Discussion

The (diphosphine)Rh(CO)$_2$H complexes of the phosphacyclic xantphos ligands are very similar to those of ligand **1** and other xantphos-type ligands. Only the (diphosphine)Rh(CO)$_2$H complex of ligand **7** behaves somewhat differently. Unlike the other complexes the (diphosphine)Rh(CO)$_2$H complex of ligand **7** does not display fluxional behavior at room temperature on the NMR time scale. The introduction of the phenoxaphosphino substituents and the *tert*-butyl-groups on the diphenyl ether backbone evidently increases the barrier for interconversion of equatorial and apical coordinated phosphines significantly. The relatively large rhodium−proton coupling constants and the relatively small rhodium−phosphorus coupling constants indicate that only the ea complex isomer is formed for ligand **7**. The relatively small phosphorus−proton constant, however, suggests that the complex is distorted to some extent. Why for ligand **2** not the (diphosphine)Rh(CO)$_2$H complex but the [(diphosphine)Rh(CO)$_2$]$_2$ dimer complex is formed exclusively under hydroformylation conditions is unclear. This may be the result of the decreased phosphine basicity (vide infra) or the wide natural bite angle. For diphosphines with rigid backbones and wide natural bite angles often an increased tendency for the formation of dimeric rhodium carbonyl complexes is observed.[7,9]

The IR spectra of the (diphosphine)Rh(CO)$_2$H complexes show that for ligands **4**−**6** the carbonyl absorptions are shifted to higher wavenumbers compared to those of the complex of ligand **1**. This indicates that the incorporation of phosphorus in six-membered rings leads to a decrease in phosphine basicity. The lower electron density on the metal results in a decrease in back-bonding of the rhodium to the carbonyl ligands, and hence, higher CO stretching frequencies are observed. This seems to be a common characteristic of the medium-sized unsaturated phosphacycles, since for the phospholes it has been reported previously that they are weaker donor ligands than their noncyclic analogues.[21] The low phosphine basicity of the phenoxaphosphine ring system may be explained by the resonance structures that can be drawn for this heterocycle.[22] Another effect of the lower phosphine basicity in combination with the wider natural bite angles is an increase of the ee:ea isomer ratio of the (diphosphine)Rh(CO)$_2$H complexes.[14] This is clearly demonstrated by comparing the NMR and IR spectra of the complexes for ligands **4**−**6** with those of the complex for ligand **1**.

Resonance structures

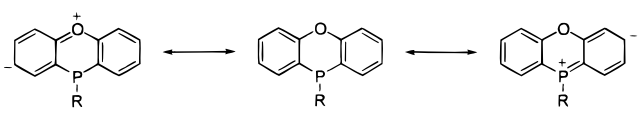

The enhancement of the hydroformylation rate observed for ligands **2**−**6** compared to ligand **1** is in agreement with earlier studies, in which phosphacyclic ligands have been applied in hydroformylation. Hayashi and co-workers have reported on the hydroformylation using dibenzophospholes and dibenzophospholyl-modified diphosphine ligands.[23−25] Two derivatives of the BISBI ligand substituted with dibenzophospholyl groups were developed independently at Eastman Kodak and Hoechst.[26,27] The phenoxaphosphine moiety has been introduced into ligands for rhodium-catalyzed hydroformylation by Hobbs and Knowles.[28] They studied the asymmetric hydroformylation of vinyl acetate with several DIOP derivatives, including one substituted with two 2,8-dimethylphenoxaphosphino groups. The general characteristic found for all these phosphacyclic ligands is that they lead to more active catalysts than their diphenylphosphino-substituted parent compounds. To the best of our knowledge, the phosphorine and phenothiaphosphine phosphacycles have not been employed in catalysis so far.

The rate enhancement that is induced by the phosphacycles may be explained by a combination of electronic and steric effects. Hayashi and co-workers have suggested that the rate acceleration observed for the dibenzophospholyl moiety can be ascribed to the higher electronic "elasticity" of the phosphacycle compared to diphenylphosphine.[24] The larger electronic "elasticity" is attributed to the extended conjugation of the ligand π-system, which supposedly buffers the charge fluctuation on rhodium along the different steps in the hydroformylation cycle more efficiently. Following this reasoning the high activity of the phenoxaphosphino moiety can be explained in a similar fashion. Like the dibenzophosphole ring, the phenoxaphosphine ring is more or less flat (the dihedral angle between the two outer rings of the phosphacycle is only 15°[22]), leading also to an extension of the conjugation of the ligand π-system.

A more common electronic explanation can be found in the phosphine basicity of the different phosphacycles. The increase of the reaction rate with decreasing phosphine basicity is generally observed in rhodium-catalyzed hydroformylation, also for the xantphos-type ligands.[14,20,29] The phosphine basicity cannot explain, however, the order of reactivity between the phosphacyclic ligands. Although the least basic diphosphine, ligand **5**, displays the highest activity, the order of reactivity between ligands **3**, **4**, and **6** is the opposite of what can be expected based on the carbonyl frequencies of the (diphosphine)Rh(CO)$_2$H complexes. The relatively modest activity of ligand **6** may be explained, however, by the higher flexibility of the phenothiaphosphine ring system or by partial coordination of the sulfur atoms to

(21) Neibecker, D.; Reau, R. *J. Mol. Catal.* **1989**, *53*, 219−227.
(22) Mann, F. G.; Millar, I. T.; Powell, H. M.; Watkin, D. J. *J. Chem. Soc., Perkin Trans. 2* **1976**, 1383−1385.
(23) Tanaka, M.; Ikeda, Y.; Ogata, I. *Chem. Lett.* **1975**, 1115−1118.
(24) Hayashi, T.; Tanaka, M.; Ogata, I. *J. Mol. Catal.* **1979**, *6*, 1−9.
(25) Hayashi, T.; Tanaka, M.; Ikeda, Y.; Ogata, I. *Bull. Chem. Soc. Jpn.* **1979**, *52*, 2605−2608.
(26) Devon, T. J.; Phillips, G. W.; Puckette, T. A.; Stavinoha, J. L.; Vanderbilt, J. J. (to Eastman Kodak) U.S. Patent 5.332.846, 1994 [*Chem. Abstr.* **1994**, *121*, 280879].
(27) Bahrmann, H.; Lappe, P.; Herrmann, W. A.; Albanese, G. P.; Manetsberger, R. B. (to Hoechst AG) EP 646.588, 1994 [*Chem. Abstr.* **1995**, *123*, 112408d].
(28) Hobbs, C. F.; Knowles, W. S. *J. Org. Chem.* **1981**, *46*, 4422−4427.
(29) Unruh, J. D.; Christenson, J. R. *J. Mol. Catal.* **1982**, *14*, 19−34.

rhodium, resulting in catalyst deactivation. The results of CO dissociation experiments show that the high activity of ligand **5**, which places it among the most active diphosphines known, can be attributed to the higher rate constant for CO dissociation. The fact that the 4-fold faster CO dissociation compared to ligand **4** only leads to approximately a 2-fold increase in hydroformylation rate is partially explained by the concomitant higher rate of isomerization observed for ligand **5**. Furthermore, the electronic factors that promote the CO dissociation can adversely affect the consecutive steps in the hydroformylation cycle.

It is remarkable that ligand **2** is also very active in the hydroformylation. Although the increased activity can also be explained by decreased phosphine basicity, the catalyst resting state for ligand **2** is the (inactive) $[(\text{diphosphine})\text{Rh}(\text{CO})_2]_2$ dimer complex and not the $(\text{diphosphine})\text{Rh}(\text{CO})_2\text{H}$ complex. The hydroformylation experiments at increased hydrogen pressure show that the reaction of dimer complex with hydrogen is not rate limiting, since the 5-fold higher pressure resulted in an increase of the activity of only 50%.

The higher activity of the phosphacyclic xantphos derivatives **2**−**6** compared to the parent ligand **1** is explained by the wider natural bite angles of the former ligands, in addition to the lower phosphine basicity. Especially diphosphines with bite angles close to 120° prove to be very active ligands.[7−9] The difference in activity between ligands **5** and **7** demonstrates that the rigidity of the ligand backbone is crucial for obtaining highly active catalysts. The rigid xanthene-based ligand **5** is more than 15 times as active as ligand **7**, which contains the more flexible diphenyl ether backbone.

Upon the introduction of the phosphacyclic moieties, the very high selectivity for linear aldehyde formation, obtained for the ligand **1**, is somewhat reduced. Despite wider natural bite angles, lower selectivities are observed for ligands **2**−**7** compared to ligand **1**. For ligands **2** and **5** the lower selectivity for linear aldehyde formation is the result of an increased isomerization rate, while for ligands **3**, **4**, **6**, and **7** it is caused by a reduced l:b ratio. These results, however, are consistent with the model that the ligand backbone determines the regioselectivity in the hydroformylation reaction by controlling the orientation of the phenyl substituents of the diphosphines.[14] In ligands **2**−**7** the orientation of the phenyl substituents of the diphosphines is fixed by the rigid phosphacycles. This results in decreased steric hindrance for the alkene entering the rhodium coordination sphere and, hence, in lower linearities. In this context it is important to note that the high l:b aldehyde ratios obtained for ligands **2** and **5** are not caused by more selective formation of the linear alkyl rhodium species, but are the result of an increased tendency of the branched alkyl rhodium species to form 2-octene. Decreasing phosphine basicity results in increasing electrophilicity of the rhodium center, which in turn leads to a higher reactivity of the rhodium species toward CO dissociation and β-hydrogen elimination.[29] Both effects were observed for ligand **5**.

The selectivities for the linear aldehyde observed for ligands **2** and **4**−**6** in the hydroformylation of 1-octene are approximately the same. This is in good agreement with the natural bite angles and the flexibility ranges of the ligands, which are comparable, and the molecular models of the ligands that predict that the steric differences between these ligands are small. The low selectivity obtained with ligand **3** is considerably out of the range obtained for the other xantphos ligands. Since the steric crowding in the rhodium complexes containing ligand **3** is expected to be considerably larger than that in the complexes of the other ligands, it is likely that at some point in the hydroformylation cycle dissociation of one of the phosphine arms occurs. This would explain not only the low selectivity but also the relatively high activity observed for ligand **3**. The low activity observed for ligand **7** is in good agreement with the observations by NMR and IR spectroscopy that only the ea isomer of the $(\text{diphosphine})\text{Rh}(\text{CO})_2\text{H}$ complex is formed for this ligand.

Very few rhodium catalysts have been reported that will hydroformylate internal alkenes at acceptable rates and even fewer that will produce linear aldehydes preferentially.[30−32] Considerable progress in this field has been made by using bulky diphosphites as modifying ligands.[33,34] The intrinsically low long-term stability of phosphites, however, warrants the development of new efficient catalysts for the hydroformylation of internal alkenes. To the best of our knowledge ligands **2** and **5** constitute the first rhodium *diphosphine* catalysts for the selective hydroformylation of internal aldehydes to linear aldehydes. The excellent performance of these ligands in the hydroformylation of internal octenes can be explained by both the low phosphine basicity and the wide natural bite angles of the ligands. The low phosphine basicity leads to the required high isomerization and hydroformylation activity, while the large natural bite angle induces the high selectivity for linear aldehyde formation. By choice of temperature and pressure the proportion between isomerization and hydroformylation activity and herewith the selectivity for linear aldehydes can be tuned. Contrary to the hydroformylation of 1-alkenes, the hydroformylation of internal alkenes toward linear aldehydes is favored by high temperature and low syn gas pressure. The absence of high isomerization activities for ligands **4** and **6** makes these ligands less suited for the selective hydroformylation of internal alkenes.

Conclusion

New phosphacyclic diphosphines with wide natural bite angles have been synthesized and a short and efficient route toward the synthesis of 10-chlorophenoxaphosphine and 10-chlorophenothiaphosphine has been developed. Upon the introduction of the phosphacyclic moieties to the xanthene backbone, the ee:ea isomer ratio of the $(\text{diphosphine})\text{Rh}(\text{CO})_2\text{H}$ complexes increases. This is the combined result of the lower phosphine basicity and the wider natural bite angles of

(30) van Leeuwen, P. W. N. M.; Roobeek, C. F. *J. Organomet. Chem.* **1983**, *258*, 343−350.
(31) van Rooy, A.; Orij, E. N.; Kamer, P. C. J.; van Leeuwen, P. W. N. M. *Organometallics* **1995**, *14*, 34−43.
(32) Breit, B.; Winde, R.; Harms, K. *J. Chem. Soc., Perkin Trans. 1* **1997**, 2681−2682.
(33) Billig, E.; Abatjoglou, A. G.; Bryant, D. R. (to Union Carbide) EP 213, 639, 1987 [*Chem. Abstr.* **1987**, *107*, 7392r].
(34) Burke, P. M.; Garner, J. M.; Tam, W.; Kreutzer, K. A.; Teunissen, A. J. J. M.; Snijder, C. S.; Hansen, C. B. (to DSM/Du Pont de Nemours) WO 97/33854, 1997 [*Chem. Abstr.* **1997**, *127*, 294939r].

the ligands. Very remarkably, for the dibenzophospholyl-substituted xantphos ligand the [(diphosphine)Rh-$(CO)_2]_2$ dimer complex is formed exclusively under hydroformylation conditions. The phosphacyclic ligands give very active and selective catalysts for the hydroformylation of 1-octene, which is also explained by the decreased phosphine basicity and the wider natural bite angles. The very high selectivity obtained employing the diphenylphosphino-substituted parent ligands, however, is slightly reduced. These results confirm the idea that the ligand backbone determines the regioselectivity of the reaction by controlling the orientation of the phenyl substituents of the diphosphines.

The phenoxaphosphino-substituted xantphos ligand proves to be one of the most active diphosphine ligands known so far. The high activity of this ligand compared to the other xantphos ligands can be ascribed to an increased rate of CO dissociation from the (diphosphine)-$Rh(CO)_2H$ complex, as determined by the rapid-scan IR experiments. The dibenzophospholyl- and phenoxaphosphino-substituted xantphos ligands constitute the first rhodium−diphosphine catalysts for the selective linear hydroformylation of internal alkenes. This area, which seemed hardly accessible before, may now be explored for a whole new range of applications for rhodium−diphosphine-catalyzed hydroformylation.

Experimental Section

Computational Details. The molecular mechanics calculations were performed using the CAChe WorkSystem version 4.0,[35] on a Apple Power MacIntosh 950, equipped with two CAChe CXP coprocessors. Calculations were carried out similarly to the method described by Casey and Whiteker,[6] using a Rh−P bond length of 2.315 Å. Minimizations were done via the block-diagonal Newton−Raphson method, allowing the structures to converge fully with a termination criterion of a rms factor of 0.0001 kcal mol^{-1} $Å^{-1}$ or less.

General Procedure. All reactions were carried out using standard Schlenk techniques under an atmosphere of purified argon. Toluene and TMEDA were distilled from sodium, THF and diethyl ether from sodium/benzophenone, and hexanes from sodium/benzophenone/triglym. Methanol, ethanol, and dichloromethane were distilled from CaH_2. Chemicals were purchased from Acros Chimica and Aldrich Chemical Co. 9-Chlorodibenzo[*b,d*]phosphole,[11] 5-chloro-1,2,3,4-tetraphenylphosphole,[11] and 10-chlorodibenzo[*b,e*]phosphorine[12] were prepared according to literature procedures. Silica gel 60 (230−400 mesh) purchased from Merck was used for column chromatography. Melting points were determined on a Gallenkamp MFB-595 melting point apparatus in open capillaries and are uncorrected. NMR spectra were obtained on a Bruker AMX 300 spectrometer. ^{31}P and ^{13}C spectra were measured ^1H decoupled. TMS was used as a standard for ^1H and ^{13}C NMR and H_3PO_4 for ^{31}P NMR. Mass spectroscopy was measured on a JEOL JMS−SX/SX102A. Elemental analyses were carried out on an Elementar Vario EL apparatus. Standard infrared spectra were recorded on a Nicolet 510 FT-IR spectrophotometer; rapid-scan (4.5 spectra per second) measurements were performed using a Bio-Rad FTS-60A spectrophotometer. HP−IR spectra were measured using a 20 mL homemade stainless steel autoclave equipped with mechanical stirring and ZnS windows. Hydroformylation reactions were carried out in a 200 mL homemade stainless steel autoclave. Syn gas (CO/H_2, 1:1, 99.9%) and CO (99.9%) were purchased from Air Liquide. D_2 was purchased from Hoekloos. ^{13}CO (99%) was purchased from Cambridge Isotope Laboratories. Gas chromatographic analyses were run on an Interscience HR GC Mega 2 apparatus (split/splitless injector, J&W Scientific, DB1 30m column, film thickness 3.0 mm, carrier gas 70 kPa He, FID detector) equipped with a Hewlett-Packard data system (Chrom-Card).

2,7-Di-*tert*-butyl-9,9-dimethyl-4,5-bis(diphenylphosphino)xanthene (Di-*t*-buxantphos, 1). At −65 °C 4.9 mL of *n*-butyllithium (2.5 M in hexanes, 12 mmol) was added dropwise to a stirred solution of 2.67 g of **8** (5.6 mmol) in 75 mL of THF. The resulting beige suspension was stirred for 1 h. Next, a solution of 2.2 mL of chlorodiphenylphosphine (12 mmol) in 10 mL of hexanes was added, and the reaction mixture was slowly warmed to room temperature overnight. The reaction mixture was diluted with 25 mL of ethyl acetate and hydrolyzed with 50 mL of a 1:1 mixture of brine and dilute hydrochloric acid. The water layer was removed, and the organic layer was dried with $MgSO_4$. The solvents were removed in vacuo, and the residual yellow oil was washed with hexanes and crystallized from ethanol/THF. Yield: 3.12 g of white crystals (81%). Mp: 194−195 °C. ^1H NMR ($CDCl_3$): δ = 7.38 (d, $^4J(H,H)$ = 2.2 Hz, 2H; $H^{1,8}$), 7.24 (m, 20H; phenyl), 6.53 (bd, $^4J(H,H)$ = 2.1 Hz, 2H; $H^{3,6}$), 1.68 (s, 6H; CH_3), 1.11 (s, 18H; *tert*-butyl). $^{31}P\{^1H\}$ NMR ($CDCl_3$): δ = −16.2. $^{13}C\{^1H\}$ NMR ($CDCl_3$): δ = 150.7 (t, $J(P,C)$ = 19.1 Hz; CO), through-space P−P coupling = 25.2 Hz, 145.4 ($C^{2,7}$), 137.0 (t, $J(P,C)$ = 13.1 Hz; PC), 134.2 (t, $J(P,C)$ = 20.4 Hz; PC*C*H), 129.7 ($C^{3,6}$), 129.1 (*C*C^9), 128.3 (d, $J(P,C)$ = 6.0 Hz; PCCH*C*H), 128.3 (PCCHCH*C*H), 124.9 (t, $J(P,C)$ = 18.9 Hz; $C^{4,5}$), 123.2 ($C^{1,8}$), 35.1 (C^9), 34.7 (*C*$(CH_3)_3$), 32.4 (C^9CH_3), 31.5 (C(*C*$H_3)_3$). IR (KBr, cm^{-1}): 2962 (s), 1477 (m), 1424 (s), 1264 (s), 1248 (m), 744 (s), 696 (s). Anal. Calcd for $C_{47}H_{48}OP_2$: C, 81.71; H, 7.01. Found: C, 81.78; H, 6.69.

4,5-Bis(9-dibenzo[*b,d*]phospholyl)-2,7-di-*tert*-butyl-9,9-dimethylxanthene (DBP−xantphos, 2). At −65 °C 8.9 mL of *n*-butyllithium (2.5 M in hexanes, 22 mmol) was added dropwise to a stirred solution of 4.85 g of **8** (10.1 mmol) in 250 mL of THF. The resulting beige suspension was stirred for 2 h. Next, a solution of 4.86 g of **9** (22.2 mmol) in 100 mL of THF was added, and the reaction mixture was slowly warmed to room temperature overnight. The reaction mixture was diluted with 250 mL of ethyl acetate and hydrolyzed with 50 mL of a 1:1 mixture of brine and dilute hydrochloric acid. The water layer was removed, and the organic layer was dried over $MgSO_4$. The solvents were removed in vacuo, and the residual white powder was washed with hexanes and crystallized from dichloromethane. Yield: 4.64 g of a white microcrystalline compound (67%). Mp: 330 °C (dec). ^1H NMR ($CDCl_3$): δ = 8.35 (dd, $^3J(H,H)$ = 7.5 Hz, $^4J(H,H)$ = 1.6 Hz, 4H; DBP−H^1), 7.97 (d, $^3J(H,H)$ = 7.5 Hz, 4H; DBP−H^4), 7.49 (dt, $^3J(H,H)$ = 7.5 Hz, $^4J(H,H)$ = 1.4 Hz, 4H; DBP−H^2), 7.41 (dt, $^3J(H,H)$ = 7.4 Hz, $^4J(H,H)$ = 1.3 Hz, 4H; DBP−H^3), 7.38 (d, $^4J(H,H)$ = 2.4 Hz, 2H; $H^{1,8}$), 6.76 (dt, $^4J(H,H)$ = 2.3 Hz, $J(P,H)$ = 2.5 Hz, 2H; $H^{3,6}$), through-space P−P coupling = 37.8 Hz, 1.69 (s, 6H; Me), 1.12 (s, 18H; *t*-Bu). $^{31}P\{^1H\}$ NMR ($CDCl_3$): δ = −20.8. $^{13}C\{^1H\}$ NMR ($CDCl_3$): δ = 151.0 (t, $J(P,C)$ = 19.6 Hz; CO), 146 ($C^{2,7}$), 144.1 (PC*C*), 142.5 (t, $J(P,C)$ = 4.5 Hz; PC), 131.9 (t, $J(P,C)$ = 26.4 Hz; DBP−C^4), 129.5 (*C*C^9), 128.7 (DBP−C^2), 127.5 (t, $J(P,C)$ = 3.0 Hz; DBP−C^3), 126.5 ($C^{3,6}$), 124.5 ($C^{1,8}$), 124.5 (m, $J(P,C)$ = 25.7 Hz; $C^{4,5}$), 121.6 (DBP−C^1), 35.1 (C^9), 34.9 (*C*$(CH_3)_3$), 33.2 (C^9CH_3), 31.6 (C(*C*$H_3)_3$).[36] IR (KBr, cm^{-1}): 3049 (m), 2962 (s), 1460 (m), 1426 (s), 1362 (m), 1264 (s), 1109 (m), 748 (s), 722 (m). Anal. Calcd for $C_{47}H_{44}OP_2$: C, 82.19; H, 6.46. Found: C, 81.66; H, 6.40.

2,7-Di-*tert*-butyl-9,9-dimethyl-4,5-bis(5-1,2,3,4-tetraphenylphospholyl)xanthene (TPP−xantphos, 3). At −65 °C 3.1 mL of *n*-butyllithium (2.5 M in hexanes, 7.8 mmol) was added dropwise to a stirred solution of 1.50 g of **8** (3.1 mmol) in 50

(35) CAChe Scientific Inc., 18700 N.W. Walker Rd., Building 92−01, Beaverton, OR 97006.

(36) Nelson, J. H.; Affandi, S.; Gray, G. A.; Alyea, E. C. *Magn. Reson. Chem.* **1987**, *25*, 774−779.

mL of THF. The resulting beige suspension was stirred for 2 h. Next, a suspension of 3.30 g of 5-chloro-1,2,3,4-tetraphenylphosphole[11] (7.81 mmol) in 75 mL of THF was added, and the reaction mixture was slowly warmed to room temperature overnight. The clear dark red reaction mixture was concentrated, and the residual brown foam was dissolved in 100 mL of DCM and washed with 25 mL of water. The water layer was removed, and the organic layer was dried over $MgSO_4$. The solvent was removed in vacuo and the resulting orange paste purified by flash column chromatography (40% DCM in light petroleum ether (v:v), $R_f = 0.55$). The product crystallized upon concentration of the eluent. Yield: 1.22 g of light yellow crystals (36%). Mp: 204−206 °C. ^{1}H NMR ($CDCl_3$): $\delta = 7.26$ (d, ^4J(H,H) = 2.7 Hz, 2H; H^{1,8}), 7.21 (d, ^3J(H,H) = 7.3 Hz, 8H; CH), 7.15 (quar., ^4J(H,H) = 2.4 Hz, J(P,H) = 2.4 Hz, 2H; H^{3,6}), 7.10 (m, 12H; CH), 6.99 (m, 8H; CH), 6.92 (m, 4H; CH), 6.84 (m, 8H; CH), 1.42 (s, 6H; Me), 1.23 (s, 18H; *t*-Bu). ^{31}P{^{1}H} NMR ($CDCl_3$): $\delta = -0.5$. ^{13}C{^{1}H} NMR ($CDCl_3$): $\delta = 148.8$, 148.6 (t, ^2J(P,C) = 12 Hz; CO), 145.7, 138.4, 137.2 (t, J(P,C) = 16.6 Hz; CP), 130.9, 130.7 (CH), 129.8 (t, J(P,C) = 8.3 Hz; CH), 128.5 (CH), 128.0 (CH), 127.8 (CH), 126.6 (CH), 126.2 (CH), 123.9 (CH), 117.0 (t, J(P,C) = 6.8 Hz), 35.5 (C^9), 34.9 (*C*(CH$_3$)$_3$), 31.6 (C(*C*H$_3$)$_2$), 30.9 (C^9*C*H$_3$). IR (KBr, cm^{-1}): 3057 (m), 2962 (s), 1599 (m), 1479 (m), 1427 (s), 1261 (s), 744 (m), 712 (m), 696 (s). Anal. Calcd for $C_{79}H_{68}OP_2$: C, 86.62; H, 6.26. Found: C, 86.34; H, 6.27.

2,7-Di-*tert*-butyl-9,9-dimethyl-4,5-bis(10-dibenzo[*b*,*e*]-phosphorino)xanthene (PCP−xantphos, 4). At −65 °C 3.2 mL of *n*-butyllithium (2.5 M in hexanes, 8.0 mmol) was added dropwise to a stirred solution of 1.75 g of **8** (3.64 mmol) in 50 mL of THF. The resulting beige suspension was stirred for 2 h and slowly warmed to 0 °C. Next 6.2 mL of zinc chloride (1.3 M in diethyl ether, 8.0 mmol) was added. After another hour a solution of 1.86 g of 10-chlorodibenzo[*b*,*e*]phosphorine[12] (8.0 mmol) in 25 mL of THF was added, and the reaction mixture was slowly warmed to room temperature. After 2 days, the reaction mixture was concentrated. The residual white paste was dissolved in 150 mL of benzene and hydrolyzed with 50 mL of a 1:1 mixture of brine and dilute hydrochloric acid. The water layer was removed, and the organic layer was dried over $MgSO_4$. The solvent was removed in vacuo, and the resulting slightly colored powder was washed with hexanes and crystallized from ethanol/THF. Yield: 2.31 g of a white microcrystalline compound (63%). Mp: 306 °C. ^{1}H NMR (C_6D_6): $\delta = 7.86$ (m, 4H; CH), 7.49 (d, ^4J(H,H) = 2.4 Hz, 2H; H^{1,8}), 7.20 (quar., ^4J(H,H) = 2.5 Hz, J(P,H) = 2.5 Hz, 2H; H^{3,6}), 7.01 (m, 12H; CH), 3.83 (AB-system: $\delta_A = 3.99$, $\delta_B = 3.67$, $^2J(H_A,H_B) = 16.6$ Hz, 4H; CH$_2$), 1.53 (s, 6H; Me), 1.08 (s, 18H; *t*-Bu). ^{31}P{^{1}H} NMR (C_6D_6): $\delta = -36.2$. ^{13}C{^{1}H} NMR (C_6D_6): $\delta = 153.6$ (d, ^2J(P,C) = 20 Hz; CO), 146.2, 141.3 (t, J(P,C) = 9.1 Hz; *C*CH$_2$), 137.2 (t, J(P,C) = 11 Hz; PC), 133.3 (t, J(P,C) = 29 Hz; PC*C*H), 131.4 (CH), 130.7, 126.5 (CH), 124.6 (d, ^1J(P,C) = 24 Hz; C^{4,5}), 124.3 (CH), 40.5 (CH$_2$), 35.7 (C^9), 34.8 (*C*(CH$_3$)$_3$), 32.3 (C^9*C*H$_3$), 31.6 (C(*C*H$_3$)$_3$). IR (KBr, cm^{-1}): 3056 (w), 2964 (s), 1461 (m), 1441 (m), 1423 (s), 1263 (s), 1244 (s), 753 (s). Anal. Calcd for $C_{49}H_{48}OP_2$: C, 82.32; H, 6.77. Found: C, 81.92; H, 6.69.

Diisopropylphosphoramidous Dichloride. At 0 °C 75 mL of diisopropylamine (0.57 mol) is added dropwise to a vigorously stirred solution of 25 mL of phosphorus trichloride (0.29 mol) in 250 mL of diethyl ether. The reaction mixture is warmed to room temperature and stirred for another 2.5 h. The white suspension is filtered, and the residual salts are washed with plenty of diethyl ether. The filtrate is concentrated and distilled at reduced pressure. Yield: 46 g of a colorless oil (79%). Bp: 86 °C (20 mbar). ^{1}H NMR ($CDCl_3$): $\delta = 3.93$ (sept., ^3J(H,H) = 6.3 Hz, 2H; CH), 1.28 (d, ^3J(H,H) = 6.9 Hz, 12H; CH$_3$). ^{31}P{^{1}H} NMR ($CDCl_3$): $\delta = 170.2$.

10-Chlorophenoxahosphine (10). At 0 °C 95 mL of *n*-butyllithium (2.5 M in hexanes, 0.24 mol) was added dropwise to a solution of 16.8 g of diphenyl ether (98.7 mmol) and 36 mL of TMEDA (0.24 mol) in 600 mL of diethyl ether/hexanes (1:2), and the reaction mixture was stirred overnight at room temperature. The resulting orange suspension was cooled to −60 °C, and a solution of diisopropylphosphoramidous dichloride in 50 mL of hexanes was added. The reaction mixture was slowly warmed to room temperature overnight. The solvents were removed in vacuo, and the residue was extracted with hexanes. The combined extracts were evaporated to dryness, and the residue was dissolved in 30 mL of phosphorus trichloride and refluxed overnight. The excess phosphorus trichloride and the formed diisopropylphosphoramidous dichloride were distilled off, and light yellow crystals of **10** were obtained after sublimation (110 °C/0.1 mbar). Yield: 12.5 g (54%). Mp: 90−91 °C. ^{1}H NMR ($CDCl_3$): $\delta = 7.83$ (ddd, ^3J(H,H) = 7.6 Hz, ^4J(H,H) = 1.7 Hz, ^3J(P,H) = 10.4 Hz, 2H; H^{1,8}), 7.58 (dt, ^3J(H,H) = 7.8 Hz, ^4J(H,H) = 1.7 Hz, 2H; H^{3,6}), 7.36 (d, ^3J(H,H) = 8.2 Hz, 2H; H^{4,5}), 7.29 (tt, ^3J(H,H) = 7.4 Hz, ^4J(H,H) = 1.3 Hz, ^4J(P,H) = 1.3 Hz, 2H; H^{2,7}). ^{31}P-{^{1}H} NMR ($CDCl_3$): $\delta = 34.5$. ^{13}C{^{1}H} NMR ($CDCl_3$): $\delta = 153.9$ (CO), 135.1 (d, ^2J(P,C) = 42.3 Hz, C^{1,8}), 133.4 (C^{3,6}), 123.8 (d, ^3J(P,C) = 12.8 Hz, C^{2,7}), 118.2 (C^{4,5}), 117.9 (d, ^1J(P,C) = 25.7 Hz, PC). Anal. Calcd for $C_{12}H_8ClOP$: C, 61.43; H, 3.44. Found: C, 61.19; H, 3.90.

2,7-Di-*tert*-butyl-9,9-dimethyl-4,5-bis(10-phenoxaphosphino)xanthene (POP−xantphos, 5). At −65 °C 3.7 mL of *n*-butyllithium (2.5 M in hexanes, 9.2 mmol) was added dropwise to a stirred solution of 2.0 g of **8** (4.2 mmol) in 50 mL of THF. The resulting beige suspension was stirred for 2 h. Next, a solution of 2.2 g of **10** (9.2 mmol) in 20 mL of toluene was added, and the reaction mixture was slowly warmed to room temperature overnight. The reaction mixture was diluted with 70 mL of dichloromethane and hydrolyzed with 25 mL of a 1:1 mixture of brine and dilute hydrochloric acid. The water layer was removed, and the organic layer was dried over $MgSO_4$. The solvent was removed in vacuo, and the resulting beige powder was washed with hexanes and crystallized from toluene. Yield: 2.23 g of a white microcrystalline compound (75%). Mp: 336−338 °C. ^{1}H NMR ($CDCl_3$): $\delta = 8.18$ (t, ^3J(H,H) = 7.2 Hz, ^3J(P,H) = 14.4 Hz, 4H; PP−H^1), through-space P−P coupling > 65 Hz, 7.40 (dt, ^3J(H,H) = 7.7 Hz, ^4J(H,H) = 1.3 Hz, 4H; PP−H^3), 7.26 (s, 2H; H^{1,8}), 7.24 (d, ^3J(H,H) = 8.2 Hz, 4H; PP−H^4), 7.17 (t, ^3J(H,H) = 7.3 Hz, 4H; PP−H^2), 6.67 (s, 2H; H^{3,6}), 1.55 (s, 6H; Me), 1.10 (s, 18H; *t*-Bu). ^{31}P{^{1}H} NMR ($CDCl_3$): $\delta = -69.9$. ^{13}C{^{1}H} NMR ($CDCl_3$): $\delta = 155.8$ (PP−CO), 149.6 (t, J(P,C) = 21.3 Hz; CO), 145.1 (C^{2,7}), 135.5 (t, J(P,C) = 43.1 Hz; PP−C^1), 130.5 (PP−C^3), 128.8 (*C*C^9), 128.5 (C^{3,6}), 125.7 (t, J(P,C) = 29.0 Hz; PP−PC), 123.8 (C^{1,8}), 123.3 (t, J(P,C) = 11.1 Hz; PP−C^2), 118.3 (C^{4,5}), 117.4 (PP−C^4), 34.4 (C^9), 34.1 (*C*(CH$_3$)$_3$), 32.7 (C^9*C*H$_3$), 30.9 (C(*C*H$_3$)$_3$). IR (KBr, cm^{-1}): 3064 (m), 2962 (s), 1583 (m), 1461 (m), 1426 (s), 1265 (s), 1224 (m), 883 (m), 758 (m). Anal. Calcd for $C_{47}H_{44}O_3P_2$: C, 78.53; H, 6.17. Found: C, 78.47; H, 5.86.

10-Chlorophenthiaphosphine (11). This compound was prepared similarly to compound **10**. Yield: 6.60 g of light yellow crystals (45%) after sublimation (100−120 °C/0.2 mbar). Mp: 121−135 °C. ^{1}H NMR ($CDCl_3$): $\delta = 7.97$ (dd, ^3J(H,H) = 7.5 Hz, ^3J(P,H) = 10.1 Hz, 2H; H^{1,8}), 7.65 (d, ^3J(H,H) = 7.2 Hz, 2H; H^{4,5}), 7.42 (m, 4H; CH). ^{31}P{^{1}H} NMR ($CDCl_3$): $\delta = 54.4$. ^{13}C{^{1}H} NMR ($CDCl_3$): $\delta = 137.8$ (d, ^2J(P,C) = 7.6 Hz, SC), 134.6 (d, ^2J(P,C) = 46.1 Hz, C^{1,8}), 133.0 (d, ^1J(P,C) = 28.7 Hz, PC), 131.0 (C^{4,5}), 128.2 (C^{3,6}), 127.2 (d, ^3J(P,C) = 12.8 Hz, C^{2,7}).

2,7-Di-*tert*-butyl-9,9-dimethyl-4,5-bis(10-phenothiaphosphino)xanthene (PSP−xantphos, 6). At −65 °C 2.6 mL of *n*-butyllithium (2.5 M in hexanes, 6.4 mmol) was added dropwise to a stirred solution of 1.40 g of **8** (2.91 mmol) in 30 mL of THF. The resulting beige suspension was stirred for 2 h. Next, a solution of 1.61 g of **11** (6.41 mmol) in 20 mL of THF was added, and the reaction mixture was slowly warmed to room temperature overnight. The reaction mixture was diluted with 40 mL of benzene and hydrolyzed with 20 mL of

a 1:1 mixture of brine and dilute hydrochloric acid. The water layer was removed, and the organic layer was dried over $MgSO_4$. The solvents were removed in vacuo, and the residual yellow oil was washed with hexanes and crystallized first from toluene and then from THF. Yield: 0.96 g of a white microcrystalline compound (44%). Mp: 307 °C. ^{1}H NMR (223 K, $CDCl_3$): δ = 8.02 (dd, ^3J(P,H) = 15.6 Hz, ^4J(H,H) = 1.9 Hz, $1H_A$; CH), 7.75 (s, $1H_A$; CH), 7.53 (m, $7H_{A/B}$; CH), 7.26 (m, $2H_A$; CH), 7.12 (m, $4H_{A/B}$; CH), 6.94 (m, $7H_{A/B}$; CH), 6.67 (t, ^3J(H,H) = 7.4 Hz, $2H_A$; CH), 6.30 (dd, ^3J(H,H) = 7.4 Hz, ^4J(H,H) = 2.9 Hz, $2H_A$; CH), 6.21 (t, ^3J(H,H) = 7.4 Hz, $2H_A$; CH), 1.86 (s, $6H_A$; Me), 7.71 (s, $2.5H_B$; Me), 1.46 (s, $9H_A$; *t*-Bu), 1.16 (s, $7.5H_B$; *t*-Bu), 1.11 (s, $9H_A$; *t*-Bu).^{1}H NMR (333 K, $CDCl_3$): δ = 7.62 (d, ^4J(H,H) = 2.3 Hz, 2H; CH), 7.36 (bm, 6H; CH), 6.88 (bs, 12 H; CH), 7.80 (s, 6H; CH_3), 1.31 (s, 18H; *t*-Bu). ^{31}P{^{1}H} NMR (223 K, $CDCl_3$): δ = −19.4 (d, J(P,P) = 9.7 Hz, $1P_A$), −33.7 (d, J(P,P) = 6.7 Hz, 1 P_A), −34.4 (s, $0.8P_B$). ^{31}P{^{1}H} NMR (333 K, $CDCl_3$): δ = −27.9 (bs, 2P). ^{13}C{^{1}H} NMR (333 K, $CDCl_3$): δ = 146.1 (d, ^2J(P,C) = 6.0 Hz, CO), 138.0 (d, ^1J(P,C) = 15 Hz, $C^{4,5}$), 135.5, 135.2, 130.2 (d, ^2J(P,C) = 14.3 Hz, CH), 129.4, 127.9 (CH), 127.0 (CH), 126.2 (d, ^3J(P,C) = 3.0 Hz, CH), 125.7 (CH), 120.3 (d, ^1J(P,C) = 15 Hz, CP), 35.2 (C^9), 34.7 ($C(CH_3)_3$), 33.4 (C^9CH_3), 31.5 ($C(CH_3)_3$). IR (KBr, cm^{-1}): 3051 (m), 2960 (s), 1453 (m), 1425 (s), 1264 (s), 1244 (m), 113 (m), 752 (s). Anal. Calcd for $C_{47}H_{44}OP_2S_2$: C, 75.17; H, 5.91; S, 8.54. Found: C, 75.06; H, 5.91; S, 8.76.

4,4′-Di-*tert*-butyldiphenyl Ether (9). This compound was prepared using a modified literature procedure.[37] At −10 °C 45 mL of *tert*-butyl chloride (0.42 mol) is added dropwise to a suspension of 32 g of diphenyl ether (0.19 mol) and 3.1 g of ferric chloride (19 mmol) in 300 mL of DCM. The reaction mixture is stirred for 2 days at 0−4 °C. The reaction mixture is washed with dilute hydrochloric acid, water, an aqueous saturated solution of sodium hydrogen carbonate, and brine. The organic layer is dried over $MgSO_4$. The solvent is removed in vacuo, and the residual light yellow oil is distilled under high vacuum. The fraction with bp 110−120 °C (1×10^{-3} mbar) was collected and crystallized twice from ethanol. Yield: 25 g of white crystals (47%). Mp: 41 °C. ^{1}H NMR ($CDCl_3$): δ = 7.38 (d, ^3J(H,H) = 8.8 Hz, 4H; CH), 7.99 (d, ^3J(H,H) = 8.8 Hz, 4H; CH), 1.41 (s, 18H; CH_3).^{13}C{^{1}H} NMR ($CDCl_3$): δ = 154.9 (CO), 145.6 ($CC(CH_3)_3$), 126.3 (CH), 118.0 (CH), 34.1 ($C(CH_3)_3$), 31.4 ($C(CH_3)_3$). IR (KBr, cm^{-1}): 2961 (s), 2866 (m), 1503 (s), 1364 (m), 1296 (m), 1237 (s), 1177 (m), 1109 (m), 829 (s). GC−MS (*m*/*z*, rel intensity): 282 (M^+, 21), 268 (21), 267 (100), 126 (11), 112 (6), 98 (21). Anal. Calcd for $C_{20}H_{26}O$: C, 85.05; H, 9.29. Found: C, 84.76; H, 9.31.

4,4′-Di-*tert*-butyl-2,2′-bis(10-phenoxaphosphino)diphenyl Ether (POP−DPEphos, 7). At 0 °C 3.5 mL of *n*-butyllithium (2.5 M in hexanes, 8.7 mmol) was added dropwise to a stirred solution of 1.02 g of 4,4′-di-*tert*-butyldiphenyl ether (3.61 mmol) and 1.3 mL of TMEDA (8.7 mmol) in 25 mL of diethyl ether. The resulting light green suspension was warmed to room temperature overnight. The reaction mixture was cooled to −60 °C, and a solution of 2.03 g of **11** (8.7 mmol) in 20 mL of benzene was added. The reaction mixture was slowly warmed to room temperature overnight. The reaction mixture was diluted with 40 mL of benzene and hydrolyzed with 20 mL of a 1:1 mixture of brine and dilute hydrochloric acid. The water layer was removed, and the organic layer was dried over $MgSO_4$. The solvents were removed in vacuo, and the residual yellow foam was washed with acetonitrile and crystallized from ethanol/toluene. Yield: 0.68 g of white crystals (28%). Mp: 187 °C.^{1}H NMR ($CD_3C_6D_5$): δ = 7.55 (bt, ^3J(H,H) = 8.1 Hz, J(P,H) = 8.1 Hz, 4H; CH), 6.98 (dd, ^3J(H,H) = 8.2 Hz, ^4J(H,H) = 1.2 Hz, 4H; CH), 6.87 (dt, ^3J(H,H) = 7.7 Hz, ^4J(H,H) = 1.6 Hz, 4H; CH), 6.71 (bt, ^3J(H,H) = 7.2 Hz, J(P,H) = 7.2 Hz, 4H; CH), 6.64 (m, 4H; CH), 5.97 (dd, ^3J(H,H) = 8.3 Hz, J(P,H) = 4.1 Hz, 2H; CH), 0.69 (s, 18H; CH_3). ^{31}P{^{1}H} NMR ($CD_3C_6D_5$): δ = −65.8. ^{13}C{^{1}H} NMR ($CD_3C_6D_5$): δ = 157.7 (d, ^2J(P,C) = 14.3 Hz; CO), 157.5 (CO), 145.0 ($CC(CH_3)_3$), 136.9 (d, ^2J(P,C) = 37.8 Hz; PC*C*H), 131.2 (CH), 130.4 (d, ^1J(P,C) = 26.4 Hz; PC), 128.9 (CH), 127.2 (CH), 123.9 (d, ^2J(P,C) = 7.6 Hz; PC*C*H), 118.7 (d, ^2J(P,C) = 5.3 Hz; PC), 118.6 (CH), 118.0 (CH), 34.0 ($C(CH_3)_3$), 31.4 ($C(CH_3)_3$). IR (KBr, cm^{-1}): 3066 (m), 2959 (s), 1583 (m), 1460 (s), 1474 (m), 1430 (s), 1264 (s), 1226 (s), 759 (s). Anal. Calcd for $C_{44}H_{40}O_3P_2$: C, 77.86; H, 5.94. Found: C, 77.68; H, 6.04.

(Di-*t*-buxantphos)Rh(CO)$_2$H (12). A solution of $Rh(CO)_2$(acac) (2.6 mg, 10 μmol) and **1** (6.2 mg, 11 μmol) in 1.0 mL of C_6D_6 was pressurized with 20 bar of CO/H_2 (1:1) and stirred for 2 h at 70 °C. After being cooled to room temperature, the reaction mixture was depressurized, transferred into a 0.5 cm NMR tube, and directly analyzed at atmospheric pressure. ^{1}H NMR (C_6D_6): δ = 7.70 (m, 6H; CH), 7.50 (d, ^4J(H,H) = 2.4 Hz, 2H; $H^{1,8}$), 7.04 (m, 2H; CH), 6.91 (m, 12H; CH), 6.69 (td, ^3J(H,H) = 6.0 Hz, ^3J(P,H) = 2.4 Hz, 2H; CH), 1.62 (s, 6H; $C(CH_3)_2$), 1.09 (s, 18H; $C(CH_3)_3$), −8.61 (dt, ^1J(Rh,H) = 6.6 Hz, ^2J(P,H) = 16.5 Hz, 1H; RhH). ^{31}P{^{1}H} NMR (C_6D_6): δ = 21.9 (d, ^1J(Rh,P) = 126.4 Hz). HP−IR (cyclohexane, carbonyl region, cm^{-1}): 2039 (m, RhCO), 1996 (w, RhCO), 1974 (m, RhCO), 1950 (m, RhCO).

[(DBP−xantphos)Rh(CO)$_2$]$_2$ (13). This compound was prepared similarly to compound **12**.^{1}H NMR (C_6D_6): δ = 7.88 (bm, 4H; CH), 7.62 (d, ^3J(H,H) = 7.8 Hz, 4H; CH), 7.33 (d, ^4J(H,H) = 2.1 Hz, 2H; $H^{1,8}$), 7.14 (t, ^3J(H,H) = 12.3 Hz, 4H; CH), 7.01 (t, ^3J(H,H) = 7.2 Hz, 4H; CH), 6.74 (bd, ^3J(P,H) = 5.4 Hz, 2H; $H^{3,6}$), 1.48 (s, 6H; $C(CH_3)_2$), 0.98 (s, 18H; $C(CH_3)_3$), −8.92 (t, ^2J(P,H) = 12.2 Hz, 1H; RhH). ^{31}P{^{1}H} NMR (C_6D_6): δ = 1.0 ($A_2A'_2XX'$-system: ^1J(Rh,P) = 149, ^2J(Rh,P) = 10, ^3J(P,P) = −16). HP−IR (cyclohexane, carbonyl region, cm^{-1}): 2010 (m, RhCO), 1981 (s, RhCO), 1797 (m, RhCORh), 1768 (s, RhCORh).

(TPP−xantphos)Rh(CO)$_2$H (14). This compound was prepared similarly to compound **12**. ^{1}H NMR (C_6D_6): δ = 7.60 (d, ^3J(H,H) = 7.5 Hz, 2H; CH), 7.47 (d, ^2J(H,H) = 6.9 Hz, 4H; $H^{1,8}$), 7.36 (m, 4H; CH), 7.18 (m, 6H; CH), 6.86 (m, 28H, CH), 1.31 (s, 6H; $C(CH_3)_2$), 1.30 (s, 18H; $C(CH_3)_3$), −8.86 (t, ^2J(P,H) = 12.2, 1H; RhH). ^{31}P{^{1}H} NMR (C_6D_6): δ = 24.2 (d, ^1J(Rh,P) = 137.9 Hz). HP−IR (cyclohexane, carbonyl region, cm^{-1}): 2028 (m, RhCO), 1980 (m, RhCO), 1947 (vw, RhCO).

(PCP−xantphos)Rh(CO)$_2$H (15). This compound was prepared similarly to compound **12**. ^{1}H NMR (C_6D_6): δ = 8.19 (m, 4H; CH), 7.44 (d, ^4J(H,H) = 2.1 Hz, 2H; $H^{1,8}$), 7.10 (m, 12H; CH), 6.96 (bs, 2H; $H^{3,6}$), 4.08 (s, 4H; CH_2), 1.39 (s, 6H; $C(CH_3)_2$), 1.07 (s, 18H; $C(CH_3)_3$), −8.92 (td, ^1J(Rh,H) = 3.9 Hz, ^2J(P,H) = 1.8 Hz, 1H; RhH). ^{31}P{^{1}H} NMR (C_6D_6): δ = −8.5 (d, ^1J(Rh,P) = 135.0 Hz). HP−IR (cyclohexane, carbonyl region, cm^{-1}): 2037 (s, RhCO), 2004 (vw, RhCO), 1981 (s, RhCO), 1958 (w, RhCO).

(POP−xantphos)Rh(CO)$_2$H (16). This compound was prepared similarly to compound **12**. ^{1}H NMR (C_6D_6): δ = 8.30 (m, 4H; CH), 7.33 (d, ^4J(H,H) = 2.1 Hz, 2H; $H^{1,8}$), 7.13 (m, 6H; CH), 7.01 (m, 6H; CH), 6.68 (bs, 2H; $H^{3,6}$), 1.37 (s, 6H; $C(CH_3)_2$), 1.07 (s, 18H; $C(CH_3)_3$), −9.14 (dt, ^1J(Rh,H) = 2.4 Hz, ^2J(P,H) = 10.4 Hz, 1H; RhH). ^{31}P{^{1}H} NMR (C_6D_6): δ = −29.0 (d, ^1J(Rh,P) = 150.7 Hz). HP−IR (cyclohexane, carbonyl region, cm^{-1}): 2048 (s, RhCO), 1988 (s, RhCO).

(POP−xantphos)Rh(^{13}CO)(CO) H (16-^{13}CO). HP ^{13}C{^{1}H} NMR (323 K, C_6D_6): δ = 198.7 (dt, ^1J(Rh,C) = 65.8 Hz, ^2J(P,C) = 16.6 Hz; Rh^{13}CO).

(PSP−xantphos)Rh(CO)$_2$H (17). This compound was prepared similarly to compound **12**. ^{1}H NMR (C_6D_6): δ = 8.07 (dquar., ^3J(H,H) = 5.4 Hz, ^3J(P,H) = 5.4 Hz, 4H; PCCH), 7.44 (d, ^4J(H,H) = 2.1 Hz, 2H; $H^{1,8}$), 7.31 (m, 6H; CH), 6.95 (t, ^3J(H,H) = 7.1 Hz, 4H; CH), 6.87 (dt, ^3J(H,H) = 7.5 Hz, ^4J(H,H) = 1.5 Hz, 4H; CH), −9.18 (dt, ^1J(Rh,H) = 3.1 Hz, ^2J(P,H) =

(37) Nowick, J. S.; Ballester, P.; Ebmeyer, F.; Rebek, J., Jr. *J. Am. Chem. Soc.* **1990**, *112*, 8902−8906.
(38) TableCurve, Jandel Scientific.

7.7 Hz, 1H; RhH). $^{31}P\{^1H\}$ NMR (C_6D_6): $\delta = -1.2$ (d, ^1J(Rh,P) = 139.8 Hz). HP−IR (cyclohexane, carbonyl region, cm^{-1}): 2044 (s, RhCO), 2010 (w, RhCO), 1985 (s, RhCO), 1963 (m, RhCO).

(POP−DPEphos)Rh(CO)$_2$H (18). This compound was prepared similarly to compound **12**. HP ^{1}H NMR (C_6D_6): δ = 8.68 (dd, J(P,H) = 13.0 Hz, ^3J(H,H) = 6.5 Hz, 2H; CH), 8.58 (dd, J(P,H) = 13.8 Hz, ^3J(H,H) = 7.4 Hz, 2H; CH), 7.94 (dd, ^3J(P,H) = 16.1 Hz, ^3J(H,H) = 7.3 Hz, 2H; CH), 7.68 (bs, 2H; CH), 6.96 (m, 4H; CH), 6.85 (t, ^3J(H,H) = 8.1 Hz, 4H; CH), 6.79 (dd, J(P,H) = 13.6 Hz, ^3J(H,H) = 7.2 Hz, 4H; CH), 5.52 (dd, J(P,H) = 8.5 Hz, ^4J(H,H) = 4.7 Hz, 2H; CH), 0.88 (s, 18H; *t*-Bu), −8.63 (td, ^1J(Rh,H) = 12.3 Hz, ^2J(P,H) = 17.3 Hz, ^2J(P,H) = 12.3 Hz, 1H; RhH). HP $^{31}P\{^1H\}$ NMR (C_6D_6): δ = −8.7 (d, ^1J(Rh,P) = 116.5 Hz), −10.3 (d, ^1J(Rh,P) = 117.3 Hz). HP−IR (cyclohexane, carbonyl region, cm^{-1}): 2014 (vw, RhCO), 2000 (s, RhCO), 1973 (vw, RhCO), 1962 (vs, RhCO).

Hydroformylation Experiments. Hydroformylation reactions were carried out in an autoclave, equipped with a glass inner beaker, a substrate inlet vessel, a liquid sampling valve, and a magnetic stirring rod. The temperature was controlled by an electronic heating mantle. In a typical experiment 50 μmol of ligand was placed in the autoclave, and the system was evacuated and heated to 50 °C. After 0.5 h the autoclave was filled with CO/H_2 (1:1) and a solution of 10 μmol of Rh(CO)$_2$(dpm) in 8.5 mL of toluene. The autoclave was pressurized to the appropriate pressure (2 or 16 bar), heated to the appropriate temperature (80 or 120 °C), and stirred for 1.5 h to form the active catalyst. Then 1.0 mL of substrate (filtered over neutral activated alumina to remove peroxide impurities) and 0.5 mL of the internal standard *n*-decane were placed in the substrate vessel, purged with 10 bar CO/H_2 (1:1), and pressed into the autoclave with 2 or 20 bar CO/H_2 (1:1). For 1-octene the reaction was stopped at the 20% conversion level by adding 0.25 mL of tri-*n*-butyl phosphite and cooling on ice. For 2-octene a sample of the reaction mixture was taken after 1 h and quenched with tri-*n*-butyl phosphite. For 4-octene the reaction was stopped after 17 h by cooling on ice. Samples of the reaction mixture were analyzed by temperature-controlled gas chromatography.

HP FT-IR Experiments. In a typical experiment the HP IR autoclave was filled with 2−5 equiv of ligand, 4 mg of Rh(CO)$_2$(acac), and 15 mL of cyclohexane. The autoclave was purged three times with 15 bar CO/H_2 (1:1), pressurized to approximately 18 bar, and heated to 80 °C. Catalyst formation was monitored in time by FT-IR and was usually completed within 1 h.

Rapid-Scan HP FT-IR Experiments. In a typical experiment the HP IR autoclave was filled with 75 μmol of ligand, 30 μmol of Rh(CO)$_2$(acac), and 15 mL of cyclohexane. The autoclave was purged four times with 15 bar of H_2, pressurized to 3 bar with ^{13}CO, and consequently to 10 bar with H_2, and heated at 40 °C for approximately 2 h. Next a gas reservoir containing 50 bar of unlabeled CO is opened, which resulted in a total pressure in the autoclave of 30 bar. At the same time the rapid-scan FT-IR experiment (270 scans min^{-1} for a total acquisition time of 2.5 min) was started.

Acknowledgment. Financial support from the Technology Foundation (STW) of The Netherlands Organization for Scientific research (NWO) is gratefully acknowledged.

OM990523J